Thermal conductivity of an ultrathin carbon nanotube with an X-shaped junction

F. Y. Meng,[1,3,*] Shigenobu Ogata,[1,2,†] D. S. Xu,[3] Y. Shibutani,[1] and S. Q. Shi[4]
[1]*Department of Mechanical Engineering, Graduate of Osaka University, 2-1 Yamadaoka Suita, Osaka 565-0871, Japan*
[2]*Center for Atomic and Molecular Technologies, Graduate of Osaka University, 2-1 Yamadaoka Suita, Osaka 565-0871, Japan*
[3]*Institute of Metal Research, Chinese Academy of Sciences, 72 Wenhua Road, Shenyang 110016, China*
[4]*Department of Mechanical Engineering, Hong Kong Polytechnic University, Hong Kong, China*
(Received 8 November 2006; published 1 May 2007)

The thermal conductivity of the ultrathin carbon nanotube with and without an X-shaped junction was investigated using nonequilibrium molecular-dynamics simulations. The ultrathin carbon nanotube exhibits superhigh thermal conductivity. The thermal conductivity of the nanotube with junctions was 20–80% less than that of a straight nanotube depending on temperature. There is a jump in the temperature profile around the junction, contributing to a larger temperature gradient and reduction in the thermal conductivity. The thermal conductivity of armchair nanotube junctions is sensitive to the topological structures at the junction region.

DOI: 10.1103/PhysRevB.75.205403 PACS number(s): 61.48.+c, 65.80.+n, 63.20.Mt, 66.70.+f

I. INTRODUCTION

With the continual miniaturization of electronic, optical, and mechanical devices, an increasing interest has been put on nanoscale materials. Carbon nanotube (CNT) multiterminal junctions (MTJs) with T, Y, and X shapes are excellent candidates for nanoscale electronic devices due to their superior combination of electronic and mechanical properties, as well as their inherent nanosize.[1–9] Significant efforts have been devoted to understanding and characterizing properties of single-walled nanotube (SWNT) MTJs, and their production and application. The thermal conductivity of nanometer materials plays a fundamentally critical role in controlling the performance and stability of nano-/microdevices, since a significant amount of heat may need to be dissipated from the nano-/microdevices to prevent structural damages. CNTs have been reported as very good candidates for efficient thermal conductors to compare with other materials,[10] with a value of 1750–5850 W/m/K by experiments[11–14] and 6600 W/m/K by calculations[15–17] due to the stiff sp^2 bond which results in a high speed of sound, together with the virtual absence of atomic defects. However, there are some defects in CNTs, such as topological defects, adsorbates, and vacancies, which affect the thermal conductivity of CNTs. Che *et al.*[18] explored the thermal conductivity of CNTs as a function of defects and vacancy concentration. Shenogin *et al.*[19] analyzed the role of chemical bonding between the matrix and the fiber on thermal transport in CNT organic matrix composites.

Multiterminal junctions can be synthesized using a template-based method or a welding method.[20–24] Based on the topology and Euler's theorem,[25,26] the structures of T-, Y-, and X-shaped junctions of CNT were proposed theoretically and their stabilities have been validated theoretically.[2,24,27,28] These junctions have a negative Gaussian curvature associated with the presence of sevenfold or eightfold rings, in contrast to fullerenes which have a positive Gaussian curvature due to the introduction of fivefold rings. All the atoms in junctions retain their sp^2 hybridization.

The ultrathin CNTs with diameters around 4 Å (Refs. 29 and 30) have been discovered soon after the discovery of CNTs by Iijima in 1991,[31] and local-density-functional calculations[32] showed that SWNTs as thin as 3.42 Å are energetically stable when exposed to the free space. The strong curvature of ultrathin CNT enhances electron-phonon coupling and makes superconductivity much more likely.[33] However, the thermal conductivity of this kind of nanotubes has not been investigated yet. In the present work, (3, 3) and (5, 0) nanotubes are chosen for this investigation.

Experimental and theoretical studies[3–7] have shown that both the symmetry of the Y junction and the chirality of the trunk and branches play a role in the rectification behavior of these structures, with the symmetry being a more significant factor. It is therefore important to know how the topological defects influence the thermal conduction properties of CNTs. Such calculations of thermal conductivity may become important for designing nanoscale devices. To the best knowledge of the authors, a thorough theoretical investigation of the thermal conductivity of X-shaped nanotube junctions has not been performed.

II. THEORY AND METHOD

In this paper, we will only consider the lattice thermal conductivity. The thermal conductivity λ along a particular direction, taken here as the z axis, is defined from Fourier's law as the heat flux J produced by the temperature gradient dT/dz, $J=(1/A)(dQ/dt)=-\lambda(dT/dz)$, where dQ is the energy transmitted across the area A in the time interval dt. A CNT is in contact with two thermal reservoirs at temperatures T_1 and T_2 at two ends, respectively (indicated by the gray regions shown in Fig. 1). The temperature of each reservoir with the length of ~0.24 nm for (3, 3) tube and ~0.42 nm for (5, 0) tube is regulated by the Langevin dynamics approach using more realistic friction and random forces.[34] The temperature difference between T_1 and T_2 is 20 K. The tube [excluding the thermal ends, denoted by L in Fig. 1(a)] is split into many equal slabs with a width of about 0.15 nm, and an average temperature gradient can be obtained by applying a linear least-squares fitting to the temperatures of these slabs. A total time of 6 ns was used for the measurement of temperature gradient. A nonequilibrium

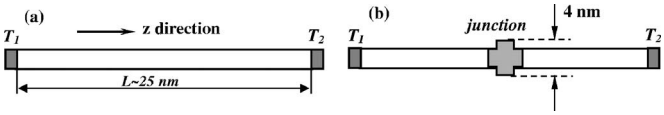

FIG. 1. (a) Simulation model for calculating the thermal conductivity of a perfect carbon nanotube and (b) a nanotube with an X-shaped junction. A temperature difference of 20 K between T_1 and T_2 is applied for the simulation. The diameter of the tube is about 0.4 nm, and the length of the junction is about 4 nm.

molecular-dynamics (MD) simulation has been performed to calculate λ using reactive empirical bond order potential.[35] Hamilton's classical equation of motion is solved using a predictor-corrector algorithm with a fixed time step of 0.5 fs. The heat exchange, determined by the kinetic energies, would be calculated when the system arrives at the steady state. The length of CNT is ~25 nm. A ring area of van der Waals thickness of 3.4 Å was employed as the cross-section area. Many processes involved in the thermal conductivity such as boundary scattering, crystal imperfections, surface effects, and isotope effects can all be included in the MD simulations.

The relaxed X-shaped junctions [denoted by the shaded cross in Fig. 1(b)] are configured in four types with different topologies, indicated by junction 1, junction 2, junction 3, and junction 4, respectively. The length of the junction is about 4 nm [shown in Fig. 1(b)]. The topological defects are present in the form of enneagons, octagons, and heptagons: (a) junction 1 with four enneagons, (b) junction 2 with 12 heptagons arranged closely, (c) Junction 3 with two heptagons and two octagons, and (d) Junction 4 with 12 heptagons arranged separately. The formation pathways for the X-shaped junction were proposed in Refs. 27 and 28. The configuration and the formation energy of each junction are summarized in Fig. 2. These junctions are stable energetically due to the negative formation energies, and the driving force for the junction formation is to partially release the strain energy of the nanotubes.[24] These junctions have a negative Gaussian curvature associated with the presence of

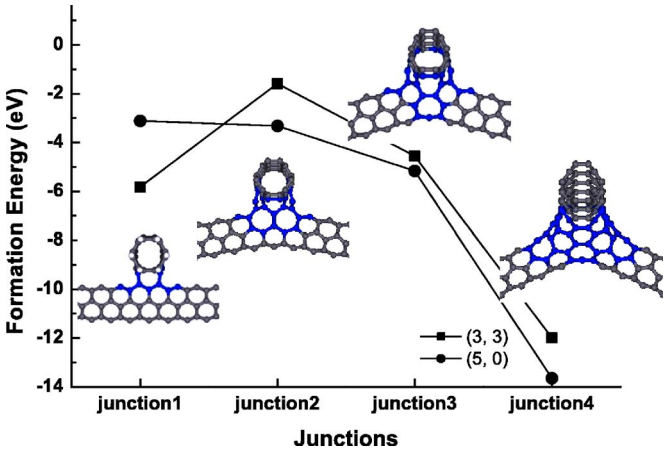

FIG. 2. (Color online) Formation energies and topological structures of the X-shaped junctions between the crossed ultrathin carbon nanotubes. Topological defects are highlighted. The detailed configurations of the junctions are specified in text.

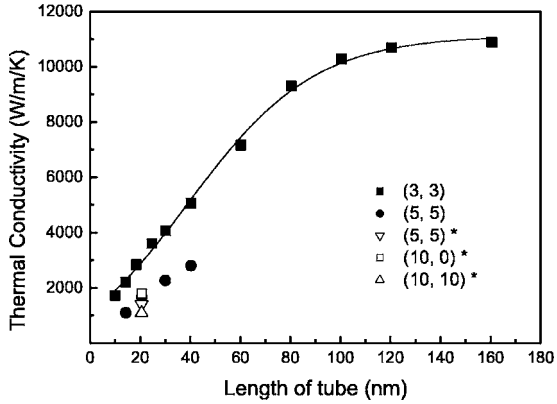

FIG. 3. Effect of the model length on the thermal conductivity of (3, 3) nanotube at 200 K. The data with a star (indicated by open symbols) are from Ref. 16.

seven-, eight-, or nine-membered rings. These junctions can be considered as a simple example of the negative-curvature structure with infinite periodic minimal surfaces,[36,37] later called schwarzites.[26] How does the X-shaped junction influence the thermal conductivity, and what is the effect of topological defects? These are important issues for the nanoscale devices composed of CNT junctions.

III. RESULTS AND DISCUSSIONS

To test the convergence of MD simulations on thermal conductivity, we carried out simulations on (3, 3) tubes at 200 K with various lengths within the range of 10–160 nm, containing 486, 690, 894, 1194, 1470, 1962, 2934, 3918, 4890, 5934, and 7824 atoms, respectively. The dependence of the calculated thermal conductivity on the tube length was shown in Fig. 3. It is found that the calculated thermal conductivity became larger and converged to a constant as the model size increased due to the boundary scattering term. The stable value of ~11 000 W/(m K) independent of the simulation size is obtained at the tube length of 120 nm. The values for (5, 5), (10, 0), and (10, 10) tubes are also given in Fig. 3 for the comparison, where the data indicated by open symbols are from Ref. 16. Superhigh thermal conductivity is shown in the ultrathin carbon nanotube. In the present report, we focus on the effect of junctions on the thermal conductivity of nanotubes. The simulation model with a length of ~25 nm was chosen to reduce the computation efforts. Comparisons were made under consistent conditions.

The results for the thermal conductivity of individual nanotubes with and without junctions over a temperature range of 50–350 K are summarized in Fig. 4. The ultrathin nanotube has superhigh thermal conductivity at high temperature because the confined geometry strongly suppresses the Umklapp process.[38] The calculated conductivity is nearly one order of magnitude larger than that of (10, 10) tube at 300 K, which verifies the expectation proposed in Ref. 39. It is also indicated that the thermal conductivity in zigzag (5, 0) tube is higher than that in armchair (3, 3) tube, which agrees with what has been reported in Ref. 40. As we expected, the X-shaped junctions with topological defects dramatically re-

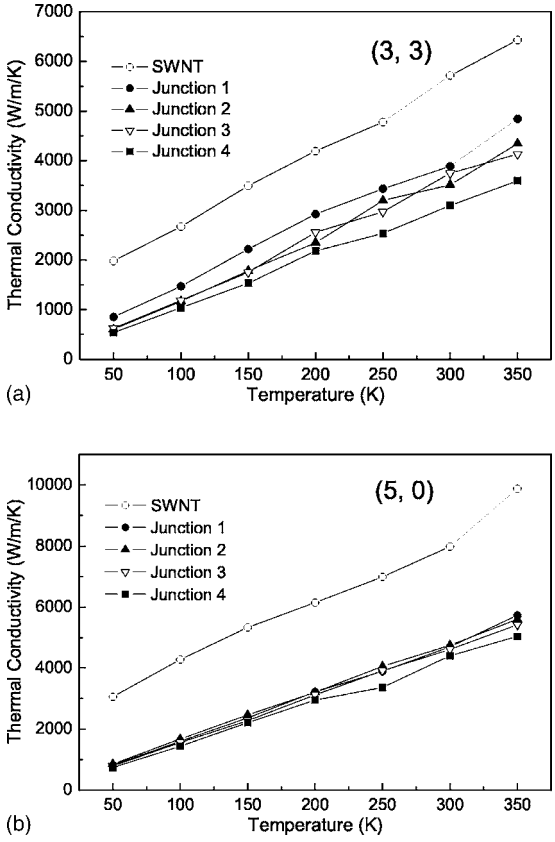

FIG. 4. The thermal conductivity of a straight tube and a tube with an X-shaped junction.

duce the thermal conductivity. For a perfect nanotube, the phonon scattering is due solely to anharmonic vibrations of atoms, while for nanotubes with junctions, the phonon scattering may be induced by topological defects around the junctions as well as by anharmonic vibrations. The conformational defects act as additional scattering centers, and therefore reduce the thermal conductivity significantly.

Figure 5 shows the dependence of the average heat flow on temperature, and Fig. 6 shows the temperature profile along the axis of the nanotubes at 100 K. The average heat

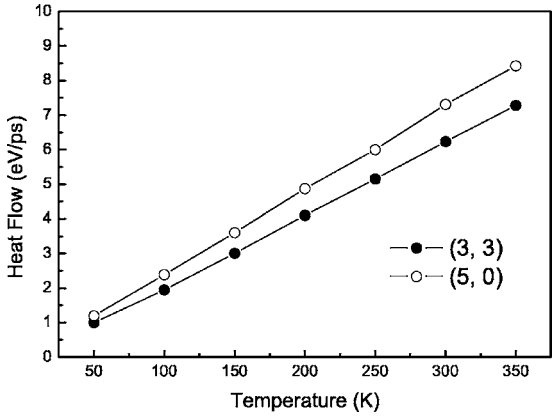

FIG. 5. The average heat flow of the (3, 3) tube and the (5, 0) tube. The heat flow of the tube with an X-shaped junction is similar to that of the corresponding straight tube.

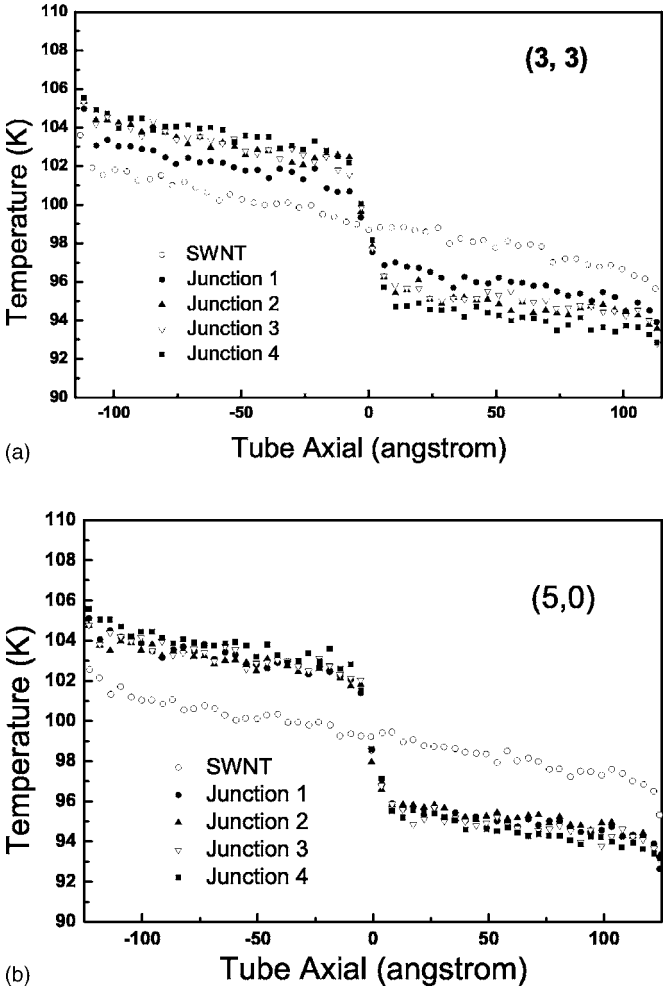

FIG. 6. The temperature profiles of the straight nanotube and the nanotube with X-shaped junctions along the tube axis at 100 K: (a) for (3, 3) tubes and (b) for (5, 0) tubes.

flow[41] of the straight tube is almost the same as that of the corresponding tube with a junction. However, there is a discontinuity in the temperature profile of tubes at junctions (Fig. 6), which shows that a junction has a much higher temperature gradient than a straight nanotube. The large temperature gradient in the local area around the junction indicates a high resistance to heat flow across the junction, leading to the reduction in the thermal conductivity of the tube with a junction at any given temperature. We always see temperature jump near the thermostat region, which can be explained by assuming a thermal boundary resistance due to the mismatch of the thermostat technique for the tube ends and the structured phonon density distribution.[42] Furthermore, the temperature jump changes with the introduction of different junctions.

The discontinuities in the temperature profile of CNTs caused by defects have been reported in the literature. Maruyama *et al.* found a jump in the temperature profile of a CNT intramolecular junction,[43] and Cummings *et al.* reported the same behavior in Y junctions.[44] The jump in the temperature profile seems to be associated with the presence of topological defects in the crystal lattice. The defects act as additional scattering centers and result in a local temperature

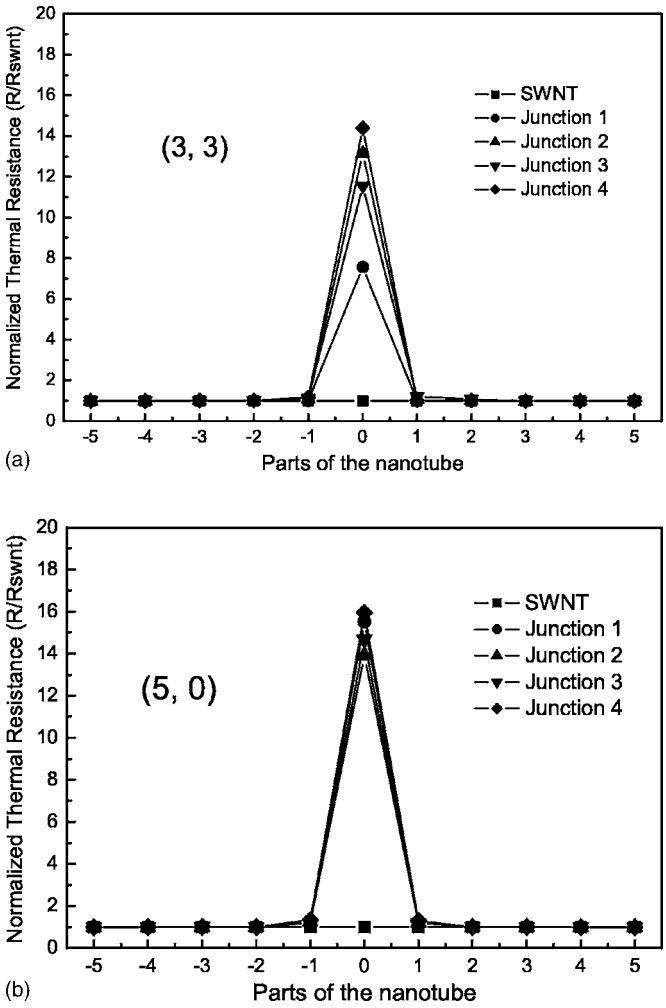

FIG. 7. The normalized thermal resistance along the tube. The junction is located in the middle of the tube.

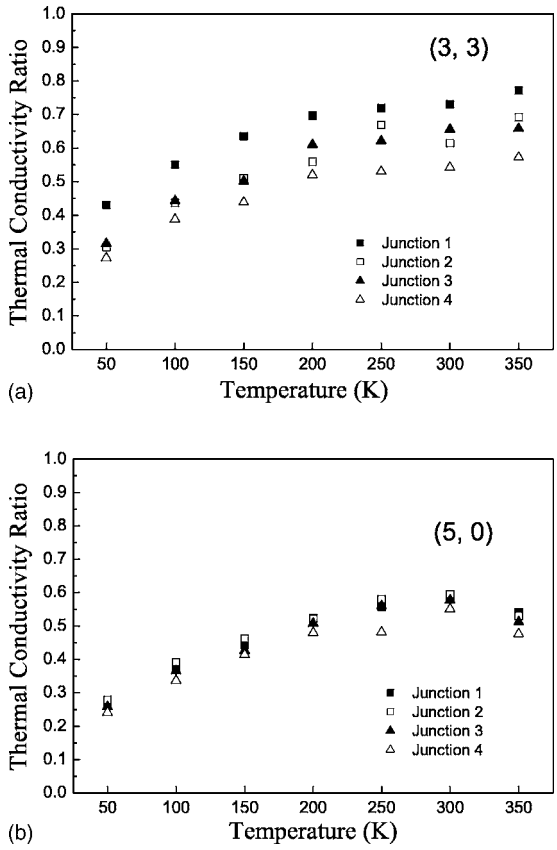

FIG. 8. Effects of the topological defects on the thermal conductivity depending on temperature.

gradient, which translates into a reduction in the thermal conductivity of the tube. Che *et al.* also reported an inverse relationship between the number of defects in a crystal and the thermal conductivity of the crystal.[18]

To clearly show the effects of the junction on the thermal conductivity independent of the length of the tube, the local thermal resistance R along the tube axis was calculated. The R is defined as $R=-\alpha[(dT/dz)/(dQ/dt)]$, where α is a constant. The local thermal resistance R is proportional to the local average temperature gradient since the heat flow is almost the same. The tube is split into 11 equal parts, and the normalized thermal resistance (R/R_{SWNT}, where R_{SWNT} is the local thermal resistance of the straight tube) was shown in Fig. 7. The junction is located at "part 0" in the abscissa (Fig. 7). It is also indicated that the introduction of the junction leads to an increase in the local thermal resistance, which is responsible for the reduction in the local thermal conductivity. Furthermore, it is implied that the effect of junction on the thermal conductivity of the zigzag tube is more severe than that in the armchair tube.

To examine the amount of decrease in thermal conductivity at the junction and the effects of geometry of junction on the thermal conductivity, we calculated the ratio of the thermal conductivity of junctions ($\lambda_{junction}$) to that of straight nanotubes (λ_{SWNT}), shown in Fig. 8. This figure indicates that the thermal conductivity of junctions decreases by 20–80%, depending on the temperature. The observation suggests that the effects of topological defects on the thermal conductivity become larger as the temperature decreases. The possible reasons are given below. Because of anharmonicity, phonons can be created, destroyed, or scattered from each other, leading to a finite phonon mean free path (MFP) and limited thermal conductivity. The phonon MFP may be affected by two factors: static and Umklapp scattering lengths.[45] Topological defects can be considered as one of the static factors. At low temperatures, the Umklapp scattering is confined since only lower-energy phonons are created; therefore, the defect scattering plays a major role in the phonon MFP. This explains why the thermal conductivity of junctions decreases greatly up to 80% compared with a perfect tube at low temperature. However, as the temperature increases, the strong phonon-phonon Umklapp scattering becomes more effective than the defects scattering when higher-frequency phonons are excited.

The thermal conductivity of armchair nanotube junctions is more sensitive to the topological defects in junctions compared with the zigzag tubes. The thin junction 1 has a higher thermal conductivity than the wide junction 4, and the medium size junctions 2 and 3 are just in the middle of the former two junctions, as shown in Figs. 7(a) and 8(a). As the junction gets wider, the scattering center becomes larger.

Therefore, more thermal scatterings happened, causing a higher thermal resistance and lower thermal conductivity. Spagnolatti *et al.*[46] and Gaito *et al.*[47] found that the topological defects affected the electron-phonon coupling, which confirms that topological configurations have effects on the thermal conductivity. The thermal conductivity may be modified by altering the geometrical configuration of junctions between the crossed nanotubes. The classical MD method is useful in describing the thermal conductivities of nanometer scale electronic and mechanical systems, since the experimental measurement on the thermal conductivity of the ultrathin nanotubes is quite challenging. Our prediction on the thermal conductivity may not be absolutely accurate due to the huge thermal gradient in the order of 10^7-10^8 K/m which makes it unlikely that the linear response theory would hold under such an extreme thermal loading condition. Nevertheless, the present work provides some useful information for future applications of ultrathin nanotubes on the electronic and mechanical devices.

IV. CONCLUSIONS

We have reported here the thermal conductivity for ultrathin CNT with and without an X-shaped junction based on MD simulations. The ultrathin CNT exhibits superhigh thermal conductivity with a value of ~11 000 W/m/K at the tube length of 120 nm to compare with the (5, 5), (10, 0), and (10, 10) tubes. The introduction of the junction gives rise to the increase of the local thermal resistance, which translates into the reduction in the thermal conductivity. The thermal conductivity of junctions decreases by 20–80% depending on the temperature compared with a straight nanotube. There is a jump in the temperature profile around the junction, contributing to a larger temperature gradient and a significant reduction in the thermal conductivity. The thermal conductivity of armchair nanotube junctions is sensitive to the topological structures at the junction region.

ACKNOWLEDGMENTS

This work was partially supported by the Japan Society for the Promotion of Science. S.O. acknowledges support by the Ministry of Education, Science, Sports and Culture, Grant No. 17760082, 2005 and the Next Generation Supercomputer Project, Nanoscience Program, MEXT, Japan. D.S.X. acknowledges the support from the National Natural Science Foundation of China (Grant No. 50471079), and S.Q.S. acknowledges the support from Research Grants Council of Hong Kong (Project No. CA04/05.SC02) and Competitive Earmark Research Grant of Hong Kong (Project No. PolyU 5306/03E).

*Electronic address: meng@comec.mech.eng.osaka-u.ac.jp
†Electronic address: ogata@mech.eng.osaka-u.ac.jp

[1] M. Menon and D. Srivastava, Phys. Rev. Lett. **79**, 4453 (1997).
[2] M. Menon, A. N. Andriotis, D. Srivastava, I. Ponomareva, and L. A. Chernozatonskii, Phys. Rev. Lett. **91**, 145501 (2003).
[3] C. Papadopoulos, A. Rakitin, J. Li, A. S. Vedeneev, and J. M. Xu, Phys. Rev. Lett. **85**, 3476 (2000).
[4] A. N. Andriotis, M. Menon, D. Srivastava, and L. Chernozatonskii, Appl. Phys. Lett. **79**, 266 (2001).
[5] A. N. Andriotis, M. Menon, D. Srivastava, and L. Chernozatonskii, Phys. Rev. Lett. **87**, 066802 (2001).
[6] V. Meunier, M. B. Nardelli, J. Bernholc, T. Zacharia, and J. C. Charlier, Appl. Phys. Lett. **81**, 5234 (2002).
[7] M. del Valle, C. Tejedor, and G. Cuniberti, Phys. Rev. B **71**, 125306 (2005).
[8] M. Terrones, F. Banhart, N. Grobert, J. C. Charlier, H. Terrones, and P. M. Ajayan, Phys. Rev. Lett. **89**, 075505 (2002).
[9] N. Hirosaki, S. Ogata, C. Kocer, H. Kitagawa, and Y. Nakamura, Phys. Rev. B **65**, 134110 (2002).
[10] F. Cleri, P. Keblinski, I. Jang, and S. B. Sinnott, Phys. Rev. B **69**, 121412(R) (2004).
[11] J. Hone, M. Whitney, C. Piskoti, and A. Zettl, Phys. Rev. B **59**, R2514 (1999).
[12] J. Hone, M. C. Llaguno, N. M. Nemes, A. T. Johnson, J. E. Fisher, D. A. Walters, M. J. Casavant, J. Schmidt, and R. E. Smalley, Appl. Phys. Lett. **77**, 666 (2000).
[13] W. Yi, L. Lu, Z. Dian-lin, Z. W. Pan, and S. S. Xie, Phys. Rev. B **59**, R9015 (1999).
[14] E. Pop, D. Mann, Q. Wang, K. Goodson, and H. J. Dai, Nano Lett. **6**, 96 (2006).
[15] S. Berber, Y. K. Kwon, and D. Tománek, Phys. Rev. Lett. **84**, 4613 (2000).
[16] M. A. Osman and D. Srivastava, Nanotechnology **12**, 21 (2001).
[17] S. Maruyama, Physica B **323**, 193 (2002).
[18] J. Che, T. Cağin, and W. Goddard III, Nanotechnology **11**, 65 (2000).
[19] S. Shenogin, A. Bodapati, L. Xue, R. Ozisik, and P. Keblinski, Appl. Phys. Lett. **85**, 2229 (2004).
[20] L. Jing, C. Papadopolous, and J. Xu, Nature (London) **402**, 253 (1999).
[21] L. P. Biró, Z. E. Horváth, G. I. Márk, Z. Osváth, A. A. Koós, A. M. Benito, W. Maser, and Ph. Lambin, Diamond Relat. Mater. **13**, 241 (2004).
[22] I. Jang, S. B. Sinnott, D. Danailov, and P. Keblinski, Nano Lett. **4**, 109 (2004).
[23] A. V. Krasheninnikov, K. Nordlund, J. Keinonen, and F. Banhart, Phys. Rev. B **66**, 245403 (2002).
[24] F. Y. Meng, S. Q. Shi, D. S. Xu, and R. Yang, Phys. Rev. B **70**, 125418 (2004).
[25] V. H. Crespi, Phys. Rev. B **58**, 12671 (1998).
[26] R. B. King, Croat. Chem. Acta **73**, 993 (2002).
[27] I. Ponomareva, L. A. Chernozatonskii, A. N. Andriotis, and M. Menon, New J. Phys. **5**, 119 (2003).
[28] F. Y. Meng, S. Q. Shi, D. S. Xu, and C. T. Chan, Modell. Simul. Mater. Sci. Eng. **14**, S1 (2006).
[29] Z. K. Tang, H. D. Sun, J. Wang, J. Chen, and G. Li, Appl. Phys. Lett. **73**, 2287 (1998).
[30] N. Wang, Z. K. Tang, G. D. Li, and J. S. Chen, Nature (London)

408, 50 (2000).
[31] S. Iijima, Nature (London) **354**, 56 (1991).
[32] I. Cabria, J. W. Mintmire, and C. T. White, Phys. Rev. B **67**, 121406(R) (2003).
[33] L. X. Benedict, V. H. Crespi, S. G. Louie, and M. L. Cohen, Phys. Rev. B **52**, 14935 (1995).
[34] J. C. Tully, Y. J. Chabal, K. Raghavachari, J. M. Bowman, and R. R. Lucchese, Phys. Rev. B **31**, 1184 (1985).
[35] D. W. Brenner, O. A. Shenderova, J. A. Harrison, B. S. J. Stuart, B. Ni, and S. B. Sinnot, J. Phys.: Condens. Matter **14**, 783 (2002).
[36] A. L. Mackay and H. Terrones, Nature (London) **352**, 762 (1991).
[37] T. Lenosky, X. Gonze, M. Teter, and V. Elser, Nature (London) **355**, 333 (1992).
[38] D. T. Morelli, J. Heremans, M. Sakamoto, and C. Uher, Phys. Rev. Lett. **57**, 869 (1986).
[39] X. H. Yan, Y. Xiao, and Z. M. Li, J. Appl. Phys. **99**, 124305 (2006).
[40] W. Zhang, Z. Y. Zhu, F. Wang, T. T. Wang, L. Sun, and Z. X. Wang, Nanotechnology **15**, 936 (2004).
[41] The average heat flow is different depending on the length of the thermal reservoir, while the temperature profile remains similar. For example, at $T=200$ K, the heat flows of (3, 3) nanotube with the thermostat lengths of 0.24, 0.73, and 1.2 nm are 4.8, 10.2, and 17.4 eV/ps, respectively, which results in different thermal conductivities, i.e., ~4100, ~10000, ~15000 W/m/K, respectively. Therefore, the absolute values of the thermal conductivity strongly depend on the boundary condition. Nevertheless, comparisons made under the same computational condition do have a great importance.
[42] D. Poulikakos, S. Arcidiacono, and S. Maruyama, Microscale Thermophys. Eng. **7**, 181 (2003).
[43] S. Maruyama, Y. Taniguchi, and Y. Shibuta, Eurotherm 75, Champagne, 2003 (unpublished).
[44] A. Cummings, M. Osman, D. Srivastava, and M. Menon, Phys. Rev. B **70**, 115405 (2004).
[45] P. Kim, L. Shi, A. Majumdar, and P. L. McEuen, Phys. Rev. Lett. **87**, 215502 (2001).
[46] I. Spagnolatti, M. Bernasconi, and G. Benedek, Eur. Phys. J. B **32**, 181 (2003).
[47] S. Gaito, L. Colombo, and G. Benedek, Europhys. Lett. **44**, 525 (1998).